

November 17th, 2011

SILMI Exchange Grant report

EXCHANGE GRANT

Reference Number : 3582

Acceptance Submitted : 05/10/2011 14:53:26

ESF ACTIVITY

Unit(s) : PESC

Activity Title : Super-intense laser-matter interactions

Activity Acronym : SILMI

PROJECT

Title of the proposed research

project : Fast Electron Transport in Diamond: Elucidating the role of solid state structure

Date of visit (starting date) : 12/09/2011

Duration : 6 week(s)

Applicant's Name : Mr. Matthias Burza, Lund, Sweden

HOST INSTITUTE(s)

Professor Paul McKenna, Glasgow, United Kingdom

Contents:

1. Scientific report
 - General Information / Summary
 - Experiment: Design and Diagnostics
 - Results assessment

2. List of Participants

1. Scientific report

General Information / Summary

A research campaign on “**Fast Electron Transport in Diamond: Elucidating the role of solid state structure**” was scheduled for the Target Area West (TAW) of the Vulcan laser facility at the Rutherford Appleton Laboratory (RAL). It was an international collaboration between researchers from Strathclyde, Sandia, RAL, Shanghai, Beijing, and Lund. PI is Paul McKenna from SUPA, Department of Physics, University of Strathclyde. From the STFC/CLF point of view however, this is a “UK campaign” with international collaborators and thus travel costs for participation from Lund are not covered.

In the present campaign, electron transport through materials, featuring various degrees of (lattice) order in their cold solid configuration was investigated by means of proton beam diagnostics. The protons are created at the target rear side mainly through a process called Target Normal Sheath Acceleration (TNSA). In this mechanism, the fast electrons, which are created during the laser solid interaction on the target front surface, set up an electric sheath at the rear surface after traversing the target after being subjected to transport dynamics plasma instabilities inside the target. The resulting modulations in the sheath field will be translated into spatial-intensity inhomogeneities of the diagnosed proton beam.

In a previous campaign [1] the same research collaboration team studied electron beam filamentation in various carbon allotropes. It was found that due to the rather quick target heating, lattice structure is maintained during TNSA, with the target remaining in a transient warm dense matter (WDM) state. This plays a major role regarding bulk conductivity and thus electron beam filamentation. Thus with increasing degree of cold state lattice order, a more uniform proton beam is observed, with lesser importance of the bulk’s conductivity at room temperature.

The present experiment will continue previous research and investigate the role of solid state structure of the target on fast electron transport in more detail. Recent simulations predict target resistivity at low temperature will have a critical role in the growth of transport instabilities and generation of collimating magnetic fields. We tested this prediction by comparing electron transport in different allotropes of carbon as an extension to the study reported in our recent PRL article [1] and also tested this prediction by comparing electron transport in initially cold targets and targets preheated isochorically using laser-accelerated proton beams.

[1] P. McKenna, A. P. L. Robinson, D. Neely, M. P. Desjarlais, D. C. Carroll, M. N. Quinn, X. H. Yuan, C. M. Brenner, M. Burza, M. Coury, P. Gallegos, R. J. Gray, K. L. Lancaster, Y. T. Li, X. X. Lin, O. Tresca, C.-G. Wahlström, 2011 Effect of Lattice Structure on Energetic Electron Transport in Solids Irradiated by Ultraintense Laser Pulses *Phys. Rev. Lett.* 106, 185004

Experiment: Design and Diagnostics

A schematic of the experimental setup can be seen in Fig 1. Beam 7 is the normal proton driver, impinging on the main target, whose structural effect on electron transport through the material is under investigation. The energy in this beam is around 100 J delivered in ~ 1 ps. Along its rear target normal, protons are accelerated as a result to the electron sheath field and various diagnostics provide a detailed picture of the sheath characteristics, which will be derived and modeled from angular proton beam charge and energy information.

As diagnostics serve stacks of radiochromatic film (RCF), a Thomson parabola, an optical beam line designed to provide information on coherent transmission radiation (CTR), optical transmission radiation (OTR), streaked optical probe (SOP) and Pyrometry. Additionally a pulsed optical probe is measuring plasma expansion at the target front side interferometrically. The probe beam passes vertically and enters a Nomarski interferometer setup located outside the chamber. In reflection, a wave front sensor and a screen provide information on reflected energy and critical surface structure and velocity. An X-ray flatfields spectrometer is supposed to reveal maintained lattice order and an X-ray pinhole camera may provide redundant information on electron the transport.

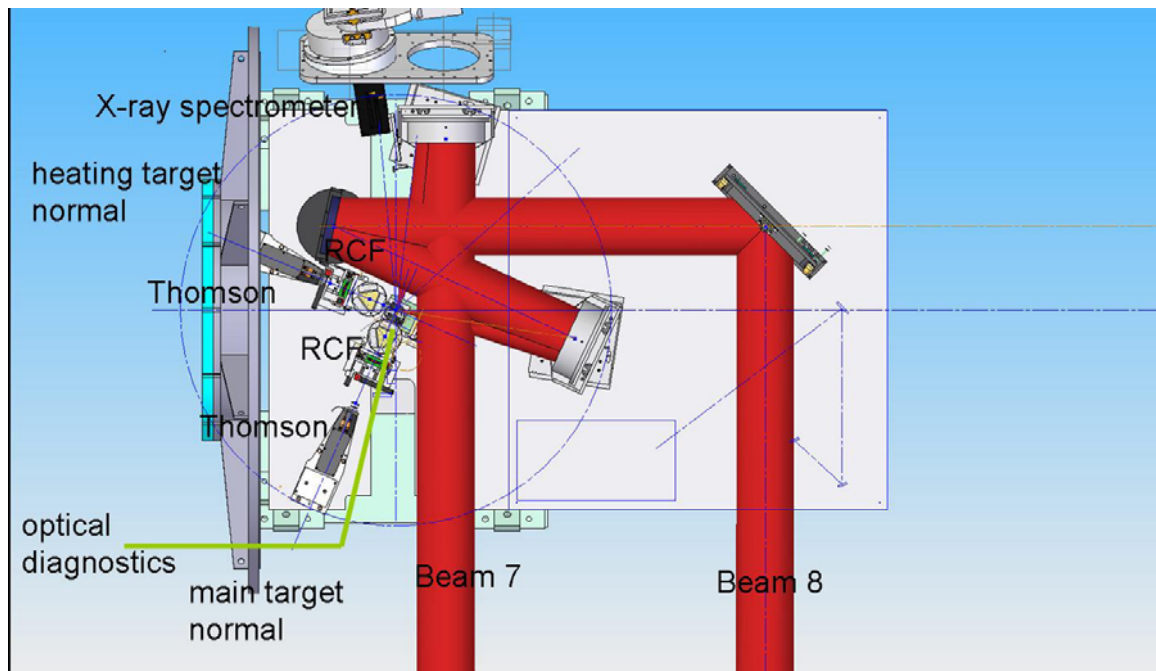


Figure 1: Target chamber setup at the Vulcan Target Area West showing major beam path and location of some diagnostics

As the major goal of the campaign is to elucidate the role of crystal structure to electron transport, complementary diagnostics are utilized to provide an as accurate picture of the emanating proton beam to accurately model the electron sheath and thus

learn something about electron transport through the target such as filamentation and charge break up.

As a major diagnostics serve rather simple and reliable RCF stacks. Comprised of multiple layers of RCF, sensitive to protons and absorption filters in between, they provide a rather complete picture of proton energy densities and beam structures over the entire ~ 30 deg divergence angle.

Thomson spectrometers are able to look in one direction only but provide very accurate information about energy and are mass to charge ratio sensitive for the accelerated particles. Thus capable of verifying the heavy ion species accelerated during TNSA.

An X-ray pinhole camera observes K-edge emission and provides a spatial image of lateral electron beam characteristics.

During the experimental campaign, the applicant was responsible for the optical diagnostics line, designing, building and driving the diagnostics during the experiment. It comprised various detectors and will provide complementary information to the RCF stacks in the data evaluation. In this diagnostics line, a $f=400\text{mm}$ focal length, 3 inch lens, images coherent optical transition radiation down the detectors. Therefore it has to be positioned as close as possible to the target rear normal as well. An ATIK 16bit CCD camera provides a direct lateral image of coherent transmission radiation (CTR) emitted from the target rear side. Interference filters ensure, that only coherent radiation in the right frequency range is penetrating down to the camera. A beam splitter and an aperture spatially filter the radiation and forward part of it to the entrance slit of a Shamrock spectrometer / Andorr camera unit. A lens slightly out of focus ensures that an integrated spectrum is acquired over the entire optical transmission radiation (OTR). The spectrum is analyzed with a high resolution grating (1200 lines/mm), with a field of view of $\sim 50\text{nm}$ at 2ω only.

Prior to the CTR/OTR diagnostics line a beam splitter will direct some unfiltered radiation onto a second Shamrock spectrometer / Andorr camera unit endowed with a small resolution grating (150 lines/mm) and a large 600 nm field of view. Spatial filtering with an aperture and a 532nm notch filter ensure that the right spectral components are analyzed with the aim to deduce a target temperature from the recorded Planck curve of the emitted thermal radiation observed from the back of the target. Another beam splitter redirects the integrated spectrum to a streak camera, where spectrally integrated emission will be recorded with time resolution. In summary, the optical diagnostics line can provide spatial and temporal and spectral resolution of coherent transmission radiation and incoherent thermal radiation.

However in experiment stacks of RCF were prioritized with the optical diagnostics line and Thomson spectrometer blocked for a substantial amount of shots.

To manipulate the main target and modifying the crystal structure, i.e. preheating it to a specified temperature prior to TNSA taking place, a secondary (heating) target, irradiated by beam line 8, which provides 300 J over 12 ps, will produce protons for isochoric

heating of the main target. By this it should in principle be possible to continuously degrade crystal structure depending on the timing between heating and main pulse. A second RCF stack provides spectral information on this heating proton beam.

K edge absorption in the main target will provide information about pertained crystal structure. Here, a third target is irradiated and its X-ray absorption through the main target is analyzed by a flat field X-ray spectrometer.

Results assessment

Even though having a large range of redundant diagnostics available, the primary diagnostics are stacks of RCF. These consist of layers of Mylar and RCF, alternatingly, so that each layer corresponds to a certain proton energy range. Depending on the deposited dose, RCF changes color from white to blue. Nonuniformities in the proton beam will be imprinted into the RCF as a color variation. FIG 2 shows a comparison between a rather smooth proton beam and a beam, where nonuniformities in the electron sheath leave their imprint in the resulting proton beam.

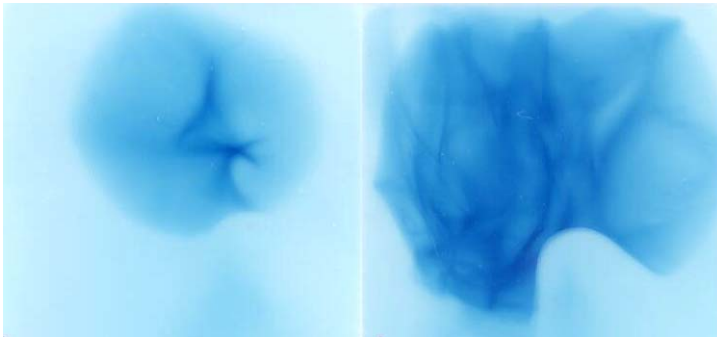


Figure 2: left: Proton beams originating from a 300 μ m thick target irradiated by a 1 ps long pulse with an energy around 70 J on target, producing an intensity of the order 10^{19} W/cm². Left: Target with highly regular crystal structure; Right: highly disordered target of same element.

This angular proton distribution can then be utilized to model the electron sheath, producing the particle beam and thus allow conclusions about electron beam breakup, filamentation and pinching of the fast electron current through the target.

Extending our previous study, we investigated vitreous Carbon and Silicon as well. Beam characteristics such as smoothness inside the beam, edge sharpness, roundness and blurs due to electron beam filamentation are assessed and will be evaluated quantitatively to model the electron sheath at the target rear. We have seen new features when probing single crystal diamond compared to what we have published in [1]. Silicon, which hasn't been studied before and which should have comparable room temperature resistivity and the same diamond lattice structure, was investigated as well. Indeed distinct differences in its resulting proton beams are visible.

The preheating with an additional TNSA laser/foil proton source has been investigated on various carbon allotropes available during this campaign and effects on structures on the beam and edge definition could be seen. Three different timings for the heating pulse have been tested and indeed structures in the RCF are modified.



11: 200 μ m vitr. C, (Al)

12: 300 μ m sg cr Diamond

13: 200 μ m flex graphite
(Al)

In this context, CTR provides redundant information to RCF about electron beam break through on the rear target surface. This will alleviate modeling of the electron beam as it provides a more direct image of the electron distribution after having traversed the target. Fig 3 to the left is an example of variation in transmission radiation, showing various degree of smoothness depending on the target material.

Fig. 3: Examples of CTR

As a conclusion, data covering all three objectives, the investigation of lattice effects on electron transport without proton heating, heating effects on fast electron transport as well as ion motion effect studies by isochoric target preheating have been acquired and will improve our understanding of the role of the lattice structure on fast electron transport. This in turn will have impact on choice of target material and target design for various applications to effectively couple laser energy into sheath accelerated protons.

2. List of Participants

<u>User Group</u>	<u>Role</u>	<u>Email Address</u>
Paul McKenna ¹	PI	paul.mckenna@strath.ac.uk
David Neely ²	Co-investigator	david.neely@stfc.ac.uk
Alex Robinson ²	Co-investigator	alex.robinson@stfc.ac.uk
Claes-Goran Wahlstrom ³	Co-investigator	Claes-Goran.Wahlstrom@fysik.lth.se
Dr M Desjarlais	Co-investigator	
David Carroll ¹	TAO	david.carroll@strath.ac.uk
David MacLellan ¹		david.maclellan@strath.ac.uk
Ross Gray ¹	DTAO	ross.gray@strath.ac.uk
Mireille Coury ¹		mireille.coury@strath.ac.uk
Haydn Powell ¹		haydn.powell@strath.ac.uk
Graeme Scott ^{1,2}		graeme.scott@stfc.ac.uk
Xiaohui Yuan ⁵		xiaohui.yuan@sjtu.edu.cn
Yuan Fang ⁵		loryin1988@sjtu.edu.cn
Fei Du ⁴		dufei@aphy.iphy.ac.cn
Mathias Burza ³		matthias.burza@fysik.lth.se
Charles Barton		charles.barton@york.ac.uk
Dan Mihai Filipescu		
Tudor Glodariu		
<u>Support</u>		
Nicola Booth ² & Margaret Notley ²	Link	
Chris Spindloe ²	Target Prep	
Pete Brummit ²	Engineering	

Affiliations

- 1) Department of physics, University of Strathclyde, SUPA, Glasgow G4 0NG, UK
- 2) Central Laser Facility, STFC RAL, Oxfordshire OX11 0QX, UK
- 3) Department of Physics, Lund University, P.O. Box 118, S-22100 Lund, Sweden
- 4) Beijing National Laboratory of Condensed Matter Physics Institute of Physics, CAS, Beijing 100190, China
- 5) Key Laboratory for Laser Plasmas (Ministry of Education) and Department of Physics, Shanghai Jiao Tong University, Shanghai 200240, China